# Green Propellant Substituting Hydrazine: Investigation of Ignition Delay Time and Laminar Flame Speed of Ethene / Dinitrogen Oxide Mixtures

Th. Kick, J.H. Starcke, C. Naumann*
Institute of Combustion Technology, German Aerospace Center (DLR),
Pfaffenwaldring 38-40, 70569 Stuttgart, Germany

**Abstract**
The combustion properties of propellants like ethene/dinitrogen oxide mixtures that have the potential to substitute hydrazine/dinitrogen tetroxide in chemical propulsion systems are investigated. In support of CFD-simulations of new rocket engines powered by green propellants ignition delay times and laminar flame speeds of ethene/dinitrogen oxide mixtures diluted with nitrogen have been measured at atmospheric and elevated pressures aimed for the validation of reaction mechanism. Furthermore, the diluents argon and carbon dioxide have been tested with respect of the influence of their chaperon efficiencies on ignition delay time.

## 1. Introduction

Hydrazine gives the best performance and reliability as a rocket fuel, but it has a high freezing point and is too unstable for use as a coolant. Hydrazine derivatives like monomethyl hydrazine (MMH) and unsymmetrical dimethyl hydrazine (UDMH) are used for spacecraft propulsion applications in different technological contexts. But all fuels have the same disadvantage: they are highly toxic. Today, hydrazine consumption for European space activities is in the order of 2-5 t per year. However, if the impact of the REACH (Registration, Evaluation, Authorisation and Restriction of Chemicals) regulation should come into full force in the upcoming years, REACH will severely restrict its use in Europe, although the propellant may remain available from current sources. Nevertheless, green propellants for European space activities are an accepted challenge for research and for technology development. Similar to research programmes in the U.S. initiated by DARPA [1-2], DLR investigates the combustion properties of propellants like ethene/dinitrogen oxide mixtures that have the potential to substitute hydrazine/dinitrogen tetroxide in chemical propulsion systems [3-4]. Data from model combustors operated at DLR's rocket propulsion test site at Lampoldshausen (Germany) in combination with investigations of fundamental combustion properties provide valuable test cases to be analysed by CFD computations, thus gaining better insights to the specific design requirements of new rocket engines powered by green propellants.

## 2. Specific Objectives

This work aims to validate a public domain reaction model for the simulation of ethane / dinitrogen oxide combustion. Ignition delay time measurements with different diluents and laminar flame speed measurements of nitrogen diluted $C_2H_4/N_2O$-mixtures at atmospheric and elevated pressures provide a comprehensive validation data basis that could help to contribute to the understanding of the combustion of green propellants and supporting CFD simulations with a validated reaction scheme.

## 3. Experiments

### 3.1. Ignition Delay Times

The experiments were carried out at DLR's shock tube facility at Stuttgart. The shock tube used has an internal diameter of 98.2 mm. It is divided by aluminium diaphragms into a driver section of 5.18 m and a driven section of 11.12 m in length. Driver and driven section are separated by a small intermediate volume establishing a double-diaphragm operation. The driver section was loaded with mixtures of helium and argon controlled by Bronkhorst mass flow controllers to achieve tailored interface conditions. The driven section was pumped down to pressures below $10^{-6}$ mbar by a turbomolecular pump. Stoichiometric mixtures of $C_2H_4$ / $N_2O$ diluted with argon, nitrogen, or carbon dioxide were prepared manometrically in stainless steel storage cylinders, which were evacuated using a separate turbomolecular pump. Gases used were delivered by LINDE AG (N2O: 99.999%, C2H4: 99.95%, diluent N2: 99.9995% (ECD), Ar: 99.9999%, CO2: 99.9993%). Dilutions of 1:5 with argon, nitrogen and a bath gas mixture containing 30% $CO_2$ / 70% Ar, and dilution of 1:2 with $CO_2$ were applied to stoichiometric $C_2H_4$ / $N_2O$ mixtures. Due to the very short deflagration-to-detonation times, the dilution reduces the dynamic load to the shock tube during the post-ignition period after shock-heating the reactive mixtures to initial pressures of $p$ = 1, 4 and 16 bar behind reflected shock waves. The shock speed was measured over three 200 mm intervals using four piezoelectric pressure gauges (PCB 113B24). The temperature and pressure behind the reflected shock wave were computed from the measured incident shock speed and the speed attenuation using a one-

* Corresponding author: clemens.naumann@dlr.de

dimensional shock model. The estimated uncertainty in reflected shock temperature is less than ±15 K for argon as bath gas in the temperature range of our measurements.

Ignition was observed by two detection methods. First, by measuring pressure profiles with piezoelectric gauges (PCB 113B24 and Kistler 603B) located at a distance of 10 mm to the end plate. Both pressure gauges were shielded by either 1 mm polyimide or RTV106 high temperature silicone rubber to reduce heat transfer and thus signal drift. Second, for determining ignition delay times, the CH* emission at 431 nm, at the same measurement plane 10 mm to the end plate (radial) and through the end plate window (axial), was selected by narrow band pass filters (Hugo Anders, FWHM = 5 nm), detected with photomultipliers (HAMAMATSU R3896) and amplified by logarithmic amplifiers (FEMTO HLVA-100). All ignition delay time values shown in this paper were determined by measuring the time difference between the initiation of the system by the reflected shock wave at the end plate and the occurrence of the CH* maximum at the side port 10 mm away (see Figure 1).

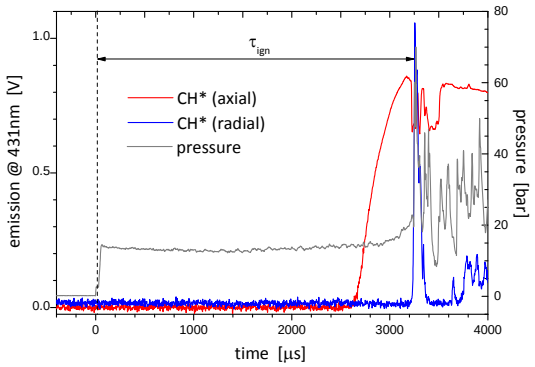


Figure 1: Pressure and emission profiles for a stoichiometric 20% ($C_2H_4$ / $N_2O$) + 80% $N_2$ mixture at initial $T$ = 1173 K and $p$ = 13.7 bar

This allows for a good comparability to simulations. Furthermore, ignition delay times were corrected by an experimentally derived blast-wave propagation time delay and were compared at the highest temperatures within each series to the end plate emission characteristics for validation. The experimental setup typically allows measurements of ignition delay times up to 8 ms depending on the temperature and the gas mixture. Nevertheless, deviations at lower temperatures, i.e. at longer ignition delay times, and at higher pressures are promoted by post-shock compression effects due to the attenuation of the reflected shock front interacting with the growing boundary layer. Usually, pressure profiles of non-reactive mixtures without distortion due to heat release provide information about the post-shock compression dynamics, and a pressure profile $p = p(t)$ can be derived to be used when modelling ignition delay times.

### 3.2. Laminar Flame Speed

A high pressure burner system was used to measure the laminar flame speed of preheated $C_2H_4$ / $N_2O$ gas mixtures diluted 1:2 with nitrogen. The experimental setup consists of the burner housing with the pressure control system, exhaust gas heat exchanger, the ignition system, and the flame holder. Calibrated Bronkhorst mass flow controllers were used for regulating fuel, oxidizer, and diluent as well as the air co-flow. The burning gases were delivered by LINDE AG (N2O: 99.95%, C2H4: 99.95%, diluent N2: 99.999%). The flame holder is made of copper and heated to 473 K. Bulk temperature and gas temperature in the plenum were monitored by type-K thermocouples. Contracting nozzles of different outlet diameters (2.0 to 8.0 mm) were used to stabilize the flame at different equivalence ratios and pressures. Typically, one change in nozzle diameter across the complete range of fuel equivalence ratios at one pressure was sufficient.

Figure 2: Photography of a conical flame for 50% ($C_2H_4$ / $N_2O$) + 50% $N_2$ at $T_{preheat}$ = 473 K, ambient pressure, and an equivalence ratio of $\varphi$ = 1.5

Digital images of the flames were captured by a CCD camera (La Vision, Imager pro) in combination with a telecentric zoom lens (Navitar, 12x). From these images, contours and cone angles were calculated by using an edge detection algorithm. Figure 2 provides a visual impression of a rich flame at ambient pressure without housing.

## 4. Modelling

As base public domain reaction mechanisms the GRI 3.0 [5] was selected and adapted to the specific needs of the reaction system. Firstly, the excited species OH* and CH* and kinetics as proposed by Smith et al. [6] and Kathrotia et al. [7] has been added. Secondly, the collision enhancement factors (CEF) for $C_2H_4$ and $N_2O$ have been estimated to CEF($C_2H_4$) = CEF($C_2H_6$) and CEF($N_2O$) = CEF($CO_2$) and supplement all reactions with collisional partners involved. Furthermore, the nitrogen reaction subset has been extended as

proposed by Powell et al. [8], and lastly, the high temperature dissociation reactions for $N_2$, NO, and CO completed the modification. This reaction model will be referred to as 'GRI3.0(ext.)'.

Modelling of the ignition delay times was performed with an adapted version of CHEMKIN II [9] with constant pressure option to ensure better comparability among the various mixtures, whereas the laminar flame speed calculations were done with Cantera's 'Free Flame' model [10].

## 5. Results and Discussion

### 5.1. Ignition Delay Time

In the following figures the results of ignition delay time measurements are presented for pressures of $p$ = 1, 4 and 16 bar and different bath gas compositions, i.e. collisional partners 'M'. Figure 3 shows the ignition delay times and modelling results for M = $N_2$. For $p$ = 1 bar the discrepancy with respect to deviation of apparent activation energy is noticeable. The deviation for low temperature measurements at $p$ = 16 bar is caused by the post-shock compression as described in section 3.1 and unaccounted for in the modelling ($p$ = *const.*). The ignition delay time reduction due to initial pressure increase is reproduced.

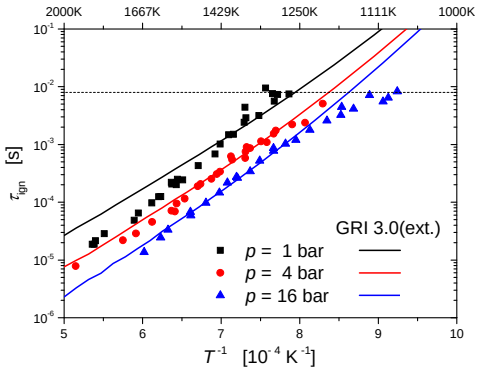


Figure 3: Ignition delay time of stoichiometric $C_2H_4/N_2O$-mixture diluted 1:5 with M = $N_2$ at initial pressures of 1, 4 and 16 bar modelled with $p$ = *const.*

Next, Figure 4 shows the ignition delay time measurements for M = Ar. The discrepancy with respect to deviation of the apparent activation energy at $p$ = 1 bar seems less pronounced than for M = $N_2$. However, monatomic argon is extremely sensitive to post-shock gas dynamics. At initial pressures of $p$ = 4 and 16 bar, the post-shock compression causes the acceleration of the reactive system towards ignition due to the dynamic temperature increase at low initial temperatures (e.g. Figure 4 for T < 1250 K).

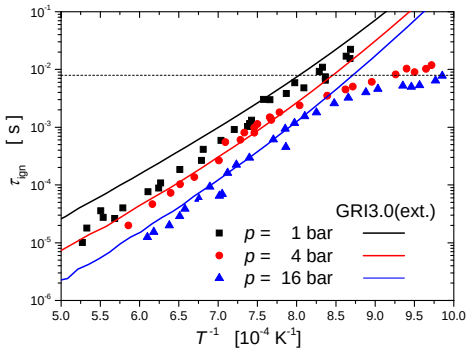


Figure 4: Ignition delay time of stoichiometric $C_2H_4/N_2O$-mixture diluted 1:5 with M = Ar at initial pressures of 1, 4 and 16 bar modelled with $p$ = *const.*

Changing the bath gas from argon to a composition consisting of 30% $CO_2$ and 70% Ar results in ignition delay times illustrated in Figure 5. Here, the reactive systems' apparent activation energy at $p$ = 1 bar seems to change at $T$ = 1500 K, i.e. $T^{-1} = 6.5 \cdot 10^{-4}$ $K^{-1}$. Moreover, the effects of post-shock compression at lower temperatures are attenuated compared to M=Ar in Figure 4.

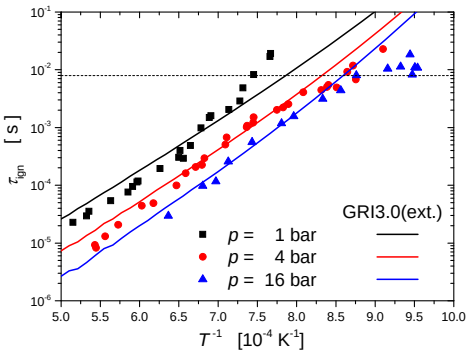


Figure 5: Ignition delay time of stoichiometric $C_2H_4/N_2O$-mixture diluted 1:5 with (30% $CO_2$ / 70 % Ar) at initial pressures of 1, 4 and 16 bar modelled with $p$ = *const.*

For a better overview, all three series at a pressure of $p$ = 1 bar and with the same dilution of 1:5 are arranged in Figure 6. The tendency of the reaction mechanism predictions with respect to the effective collision efficiency of the bath gases, i.e. CEF(30% $CO_2$ + 70% Ar) > CEF($N_2$) > CEF(Ar), seems to be reproduced by the experiments, although the slopes are deviating.

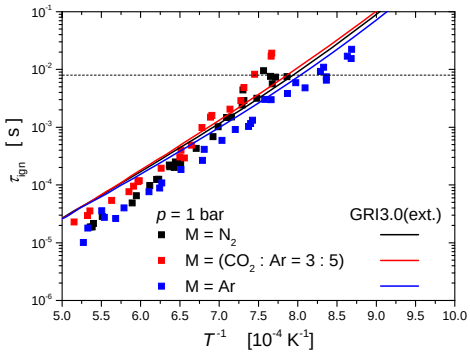


Figure 6: Ignition delay time of stoichiometric $C_2H_4/N_2O$-mixtures diluted 1:5 with different collisional partners M at initial pressure of 1 bar modelled with $p$ = *const.*

In addition to the mixtures diluted 1:5, Figure 7 shows the results of an experimental series at pressures of $p$ = 1, 4 and 16 bar with M = $CO_2$ as bath gas at a dilution of 1:2. Obviously, the scatter of the measurements has increased, especially at $p$ = 1 bar. But the abrupt change of slope, only indicated for M = (30% $CO_2$ + 70% Ar) in Figure 6, is now clearly observable. If this interpretation can also explain the trends at lower temperature for initial pressures of $p$ = 4 and 16 bar has not been confirmed yet. Measurements at a dilution of 1:5 are planned to clarify this.

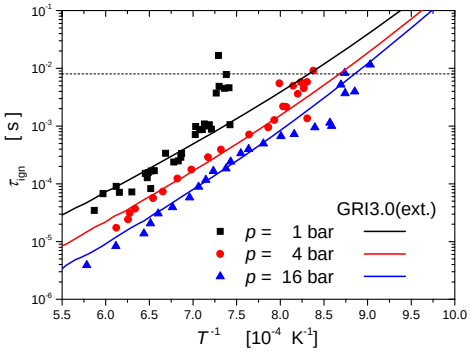


Figure 7: Ignition delay time of stoichiometric $C_2H_4/N_2O$-mixture diluted 1:2 with M = $CO_2$ at initial pressures of 1, 4 and 16 bar modelled with $p$ = *const.*

### 5.2. Laminar Flame Speed

Laminar flame speeds of $C_2H_4/N_2O$-mixtures have been measured at a dilution of 1:2 with nitrogen and at a preheat temperature of 473 K. Increasing the preheat temperature to 473 K anticipated the expected heat transfer to the nozzle, at least for pressures of $p$ = 1 and 3 bar. At a pressure of $p$ = 6 bar, compensation due to the nozzle's bulk material was not sufficient any more. Although not measureable in the bulk, heat transfer to the outmost rim of the nozzle's exit seemed to have increased the unburned gas temperature above 473 K, so that laminar flame speeds at $p$ = 6 bar overlapped with those at $p$ = 3 bar as can be noticed in Figure 8.

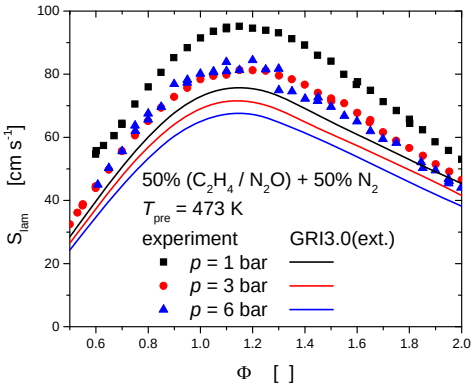


Figure 8: Laminar flame speed experiments and modelling with GRI3.0(ext.) $p$ = 1, 3 and 6 bar with M = $N_2$); at $p$ = 6 bar heat transfer to the nozzle increases gas preheat temperature above 473 K.

The predictions of the extended GRI3.0 reaction mechanism 'GRI3.0(ext.)' can also be seen in Figure 8. As expected from the comparison with the ignition delay time measurements for M = $N_2$ at $p$ = 1 bar (see Figure 3) simulated laminar flame speeds are too slow. Also for $p$ = 3 bar predicted laminar flame speeds are too slow compared with the measurements. If the measurements at $p$ = 3 bar already suffer from excess heat transfer—as those at $p$ = 6 bar do—cannot be denied unambiguously. But the trend of the measurements starting at $p$ = 1 bar to $p$ = 3 bar does not support this.

## 6. Conclusions

This contribution reports on the ignition delay and laminar flame speed measurements of diluted $C_2H_4/N_2O$ – mixtures. Initial pressures for ignition delay time measurements were $p$ = 1, 4 and 16 bar, whereas laminar flame speeds were measured at pressures of $p$ = 1, 3 and 6 bar, resp. Diluents for the ignition delay time measurements were nitrogen, argon, and a mixture of 30% $CO_2$ and 70% Ar, all at a dilution of d = 1 : 5, whereas carbon dioxide was applied at a dilution of d = 1 : 2. For the laminar flame speed measurements nitrogen at a dilution of d = 1 : 2 was used.

The GRI 3.0 reaction model has been extended with respect to collision enhancement factors and, amongst others, within a subset of sensitive nitrogen reactions according to the work of Powell et al. [8], referred to as 'GRI3.0(ext.)'. Despite of this, predictive capability with respect to laminar flame speed remained poor. With respect to ignition delay time, largest deviations remain for stoichiometric mixtures at a pressure of $p$ = 1 bar.

The result with respect to the validation targets (a) ignition delay times at $p$ = 1, 4 and 16 bar and (b) laminar flame speed at $p$ = 1 bar are not sufficiently good, so that improvement of the gas phase reaction model is the next step towards CFD combustor simulations. In addition, further investigations on high temperature hydrocarbon / nitrous oxide reaction systems and species are recommended to improve our knowledge on the elementary reaction kinetics and thermodynamics involved.

**Acknowledgements**

The authors thank Juan Ramon Diaz Moralejo, Abhishek Verma, Helena Eulalia Cano Fornos, Alexander Vollmer, and Bhaskar Bhatia for their support carrying out the experiments.

**References**

[1] N. Tiliakos et al., Development and Testing of a Nitrous Oxide / Propane Rocket Engine, AIAA 2001-3258 (2001).

[2] AEROSPACE DEFENSE MEDIA GROUP, Intelligent Aerospace, ALASA (Airborne Launch Assist Space Access): DARPA works with five aerospace companies to develop inexpensive launch capability for small satellites (2012), URL: http://www.intelligent-aerospace.com/articles/2012/06/darpa_works_withfiveaerospacecompaniestodevelopinexpensivelaunch.html (accessed 2017/01/01).

[3] L. Werling, B. Hochheimer, A. Baral, H. Ciezki, S. Schlechtriem, Experimental and Numerical Analysis of the Heat Flux Occurring in a Nitrous Oxide / Ethene Green Propellant Combustion Demonstrator, AIAA 2015-4061 (2015).

[4] L. Werling, A. Hauck, S. Mueller, H. Ciezki, S. Schlechtriem, Pressure Drop Measurement of Porous Materials: Flashback Arrestors for a N2O / C2H4 Premixed Green Propellant, AIAA 2016-5094 (2016).

[5] G.P. Smith, D.M. Golden, M. Frenklach,N.W. Moriarty, B. Eiteneer, M. Goldenberg, C.T. Bowman, R.K. Hanson, S. Song, W.C. Gardiner Jr., V.V. Lissianski, Z. Qin. Gas Research Institute (2000), URL: http://www.me.berkeley.edu/gri_mech/ (accessed 2017/01/29).

[6] G.P. Smith, J. Luque, P. Chung, J.B. Jeffries, D.R. Crosley, Low Pressure Flame Determinations of Rate Constants for OH(A) and CH(A) Chemiluminescence, Combustion and Flame 131 (2001) 59-69.

[7] T. Kathrotia, U. Riedel, A. Seipel, K. Moshammer, A. Brockhinke, Experimental and numerical study of chemiluminescent species in low-pressure flames. Applied Physics B, 107 (2012) 571-584. DOI: 10.1007/s00340-012-5002-0.

[8] O.A. Powell, P. Papas, C. Dreyer (2009), Laminar burning velocities for hydrogen-, methane-, acetylene, and propane-nitrous oxide flames, Comb.Sci.Tech. 181 (2009) 917-936.

[9] R.J. Kee, F.M. Rupley, J.A. Miller, Chemkin-II: A Fortran chemical kinetics package for the analysis of gas-phase chemical kinetics, Report No. SAND89-8009, Sandia National Laboratories (1989).

[10] D.G. Goodwin, H.K. Moffat, R.L. Speth, Cantera: An object-oriented software toolkit for chemical kinetics, thermodynamics, and transport processes (version 2.2.1) (2016). URL: http://www.cantera.org (accessed 2017/01/01).